Digest Journal of Nanomaterials and Biostructures Vol. 7, No. 3, July - September 2012, p. 973 - 982

NANO POROUS SILICON MICROCAVITY OPTICAL BIOSENSOR DEVICE FOR GLUCOSE DETECTION

P. N. PATEL[a], V. MISHRA[b*], A. K. PANCHAL [c]
[a,b]*Electronics Engineering Department,*
[c]*Electrical Engineering Department, S. V. National Institute of Technology, Surat-395007, Gujarat, India*

Recently, Porous Silicon (PS) is emerged as a new, unique and promising nano material for the optoelectronic devices and the sensing applications. In this study, rapid, sensitive, and reversible sensing of glucose level using one dimensional (1D) Porous Silicon (PS) Microcavity (MC) sensor device is successfully demonstrated.1D-PSMC sensor device structure was fabricated by electrochemical anodization of crystalline silicon wafer and proposed as a large surface area matrix for optical sensing of glucose concentrations. The refractive index of the 1D-PSMC structure is tuned by changing current density and the thickness by etching time. Wavelength shift ($\Delta\lambda$) in the measured reflectance spectra of prepared structures were analyzed for the detection of the glucose concentrations in the porous structure. Sensor device showed excellent sensing ability and good linear relation between the different concentrations of glucose and the wavelength shift. It was also observed that, the photonic resonance dip in the reflectance spectra of the 1D-PSMC sensor device promptly returned to their original states after removal of glucose molecules from the porous structure. This is a very good quality of these structures, as it is helpful in the development of reversible sensing devices.

(Received April 4, 2012; Accepted July 10, 2012)

Keywords: Nano Porous silicon; Microcavity Structures; Optical Sensor; Glucose Biosensor Device

1. Introduction

A. Glucose Background

The simple sugar is the chief source of energy. Glucose is found in the blood and is the main sugar that the body manufactures. The body makes glucose from protein, fats, and carbohydrates of food. Glucose is the primary fuel used by most cells in the body to generate the energy that is needed to carry out cellular functions (http://www.medterms.com). When glucose levels fall too low (hypoglycemic) levels, cells cannot function normally, and symptoms develop such as nervousness, cool skin, headache, confusion, convulsions or coma. High blood glucose levels (hyperglycemia) causes damage to the eyes, kidneys, nerves and blood vessels. It is comparatively easy to detect high glucose level but a low glucose level (hypoglycemia) is difficult to detect and it can lead to fainting, coma, and even death. Hence, it is demands of industry to develop the low level glucose sensors. Till date, there various techniques are reported for the glucose detection [1-4].

* Corresponding author: vive@eced.svnit.ac.in

B. History of Porous Silicon in Brief

Optical sensor field is motivated by the expectation that it has significant advantages [5] compared to conventional electronic-based sensors. In recent years, PS is emerged as a promising nano structure due to tremendous advantages like easy fabrication technology, spongy skeleton, controllable pore size and morphology etc [6]. Also, its optical properties [7] are highly sensitive to the presence of chemical and biological species inside the pores. These advantages make PS suitable in nano scale optical sensing applications. Microcavity structures are periodic dielectric structures that control the propagation of electromagnetic wave through the photonic crystals [8]. The structural properties of 1D-PSMC exhibits the sharp photonic resonance dip in the reflectance spectra which is useful for the optical sensor applications. Several groups all over the world have been working in the research related to characterization, devices, sensors and other emerging and future nano scale applications using PS [9-17].

The objective of this work is to evaluate the feasibility for realization of 1D-PSMC sensing matrix device structure by electrochemical anodization. In section 1, experimental details for the fabrication of 1D-PSMC sensing device structure is presented with materials, apparatus, fabrication procedure and sample preparations. Section 2, describes, the principle of optical sensing using 1D-PSMC, structural and optical characterization of sensing device. Finally, realization of glucose biosensor with different concentrations with the optical sensor device has been studied by examining the wavelength shift in their reflectance spectra.

2. Experimental

A. Materials

Boron-doped, one-side polished p-type silicon wafers (<100> orientation, 0.0-0.02 cm^2) were purchased (M/s. Scientific Technologies, Delhi, India). The solution for the piranha cleaning of wafer was composed of H_2SO_4 (98%, Finar Chemicals Ltd.) and H_2O_2 (30%, Fisher Scientific Ltd.).The electrochemical anodizing solution consisted of hydrofluoric acid (48%, Rankem, India) and ethanol (99.5%, Fisher Scientific, India). Analytical grade glucose (Fisher Scientific) is used. DI water was used for the dilution as well as for the rinsing purpose.

B. Apparatus

The experimental setup is shown in Fig. 1 (a). The 1D-PSMC fabrication was performed in the fume hood (Fig. 1 (a)) containing the electrochemical etching cell [9] shown in the Fig. 1 (b). As shown in Fig. 1 (b), the base and the cap of the electrochemical etching cell were made with SS 320 metal. The electrolyte mixture was kept in the highly HF resistant polymer polytetrafluoroethylene (PTFE/Teflon). Platinum grid was used as a cathode. Programmable DC power supply (PWS 4305, Tektronix) was used to generate periodic constant current square wave.

a

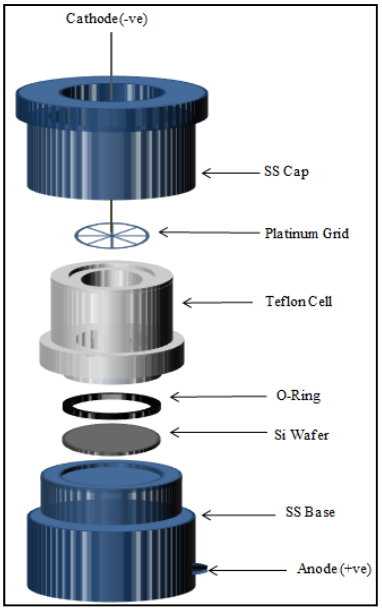

b

Fig. 1(a) Experimental Set Up, (b): Electrochemical Etching Cell

The structural morphology of the PSMC sensor device was characterized by scanning electron microscopy (FEG SEM, JSM-7600, JEOL). An UV-Vis-NIR Spectrophotometer (Maya Pro 2000, Ocean Optics Inc.) was used for the reflectance measurements of the prepared sensor device structures (Fig. 2). As shown in the Fig. 2, sensor device is illuminated with halogen lamp through a Y-shaped bifurcated fiber probe which has the central fiber providing incidence light and a bundle of six fibers around the central fiber to collect the reflected light. The reflected light is analyzed by spectrophotometer with a wavelength range of 200-100 nm with resolution of 0.5 nm. Finally, the reflectance spectrum is displayed on computer screen.

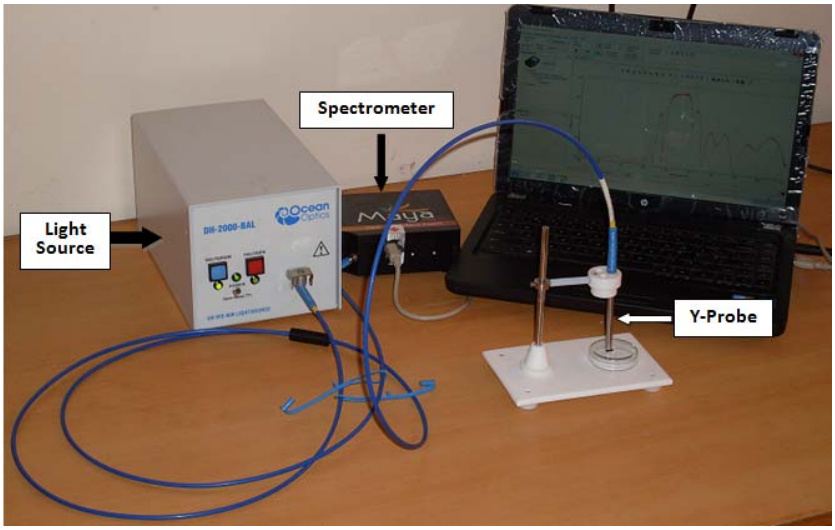

Fig. 2: Optical Spectrometer with Light Source and Accessories

C. Fabrication of PSMC Sensor Device

1D-PSMC sensor structure was fabricated using an anodization process in the electrochemical etching cell using silicon wafer. The oxidized layer of the silicon wafer was removed by standard piranha cleaning method. After, piranha cleaning, wafer was rinsed with DI water, dried at room temperature and placed inside the base of the cell, sealed with an O-ring and exposed to the electrolyte. PTFE bath was filled with the etching solution of 40% aqueous HF and 99% ethanol, mixed in the ratio of 1:2. The cathode was immersed in the electrolyte solution and the distance between anode and cathode was kept about 4.5 cm. Periodic constant current square wave was applied by programmable DC power supply. A constant current mode was used for anodization process as it is beneficial in terms of regulation [18]. Applied current density (J) and the etching time (t) profile are responsible for the change in refractive index (n) and the physical thickness (d) profile of the layer, respectively. The fabrication schematic diagram of the 1D-PSMC structure is shown in Fig. 3. In Fig. 3, n_s is the refractive index of the substrate and N is the number of period. The 1D-PSMC structure was realized by inserting a cavity layer of high current density between two identical DBR1 and DBR2 with six repetitions of a current density and etching time sequences as shown in Fig. 3.

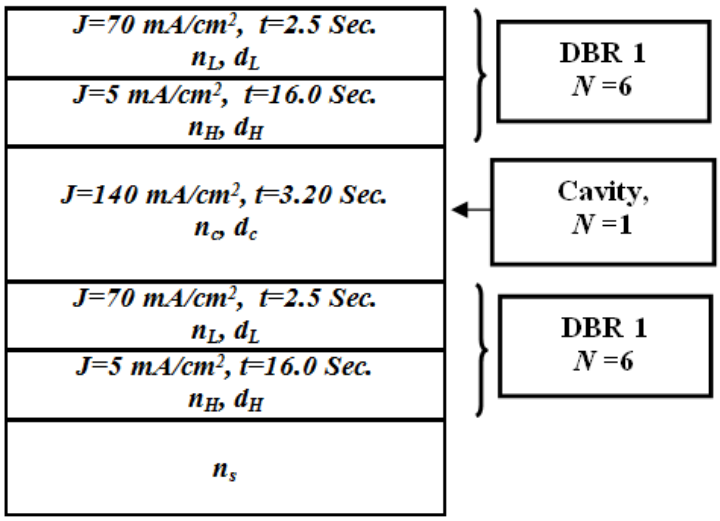

Fig. 3: Fabrication Schematic of PSMC Structure

D. Sample Preparation

In order to examine the optical response of the sensor device to glucose, glucose solutions were prepared in DI water for the different concentrations from 2% to 10% and sonicated to get a homogeneous mixture. Then the solution was dropped on to the 1D-PSMC biosensor device, hence the solution is reach to the pores of the sensor device by capillary adsorption. The amount of solution and the time of reaction were optimised to 5 µl and 30 seconds, respectively, for the reaction to be in the linear region. After the measurements, the device was thoroughly rinsed in the ethanol solution for complete removal of all the glucose molecules from the pores.

3. Results and discussion

A. Principle of Optical Sensing

According to the optics theory, the reflectance spectrum of 1D-PSMC structure is governed by the interferometric Fabry-Perot relationship [19-20]. Light reflected from the top interface (air-PS) and the bottom interface (PS-Si substrate) interfere with each other and form the typical Fabry-Perot fringes in the reflectance spectrum. The fringe pattern is closely related to effective optical thickness, which is product of physical thickness and refractive index of the structure, by the relationship shown in as:

$$m\lambda = 2nd \tag{1}$$

where, m is an integer (the spectral peak order) and λ is the peak wavelength. For bare 1D-PSMC structure (without any analyte), the refractive index of the structure is n. When the pores are filled with an analyte (e.g., chemicals or bio-chemicals), the effective refractive index of the structure increases from n to $n+\Delta n$ with shift in wavelength from λ to $\lambda+\Delta\lambda$ in the reflectance spectra due to increased optical thickness of the structure. Hence, by analyzing the wavelength shift in the reflectance spectra, capture and the detection of the analyte is done. For the multilayer 1D-PSPM structures with alternating high refractive index layers and low refractive index layers the Eq. (1) becomes:

$$\frac{m\,\lambda_0}{2} = n_L d_L \; + \; n_H d_H \tag{2}$$

where, λ_0 is the photonic resonance wavelength, n_L and d_L are the refractive index and the thickness of the low index layer, respectively, while n_H and d_H *are* the refractive index and the thickness of the high index layer, respectively.

B. PSMC Characterization

After electrochemical etching, these structures were rinsed in DI water for 10 minutes and dried at room temperature. The prepared structures show distinct green, blue and red colours distribution over the entire surface (Fig. 4). Porous structure in the bulk silicon is strongly responsible for the change in the surface colour due to the shifting in the bandgap energy of silicon [21].

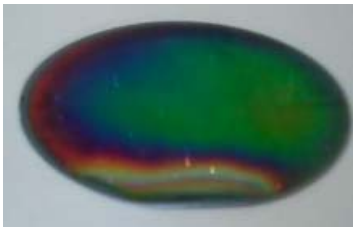

Fig. 4: Fabricated 1D-PSMC Sensor Device Structure.

Structural morphology (plan and cross sectional view) was examined by SEM. Fig. 5 (a) shows the surface morphology of the structures in SEM plan view. The array of void spaces (dark) in silicon matrix (bright) can be seen clearly in the plan view SEM image. The morphology of the structure shows that the electrochemical etching is done uniformly on the surface and created the granular structure in a spherical shape. Large number of pores distributed in all direction can be observed in Fig. 5 (a) with mean pore size of 24 nm measured using Image J software (http://rsb.info.nih.gov.ij).

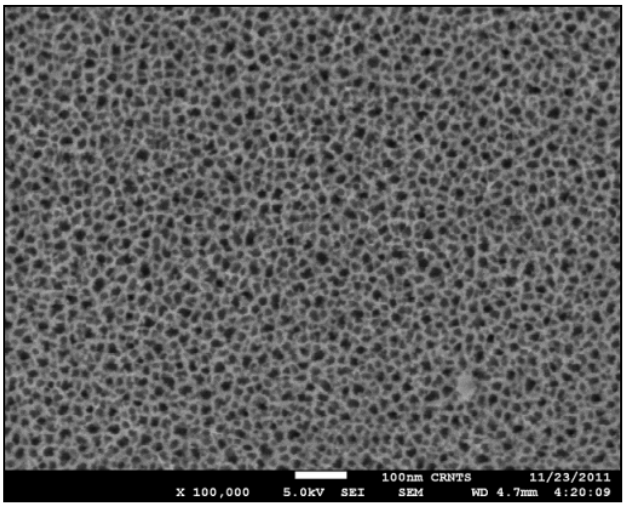

Fig. 5 (a): SEM Plan View of 1D-PSMC Structure

The SEM cross-sectional image of the 1D-PSMC structure is shown in Fig. 5 (b) and (c), respectively. Multilayered stacks are clearly observed in these figures. These stacks are due to the periodic variation in the refractive index profile through the current density variation for different etching time. The cavity layer of the microcavity structure can be clearly observed in the inset figure of Fig. 5 (b).

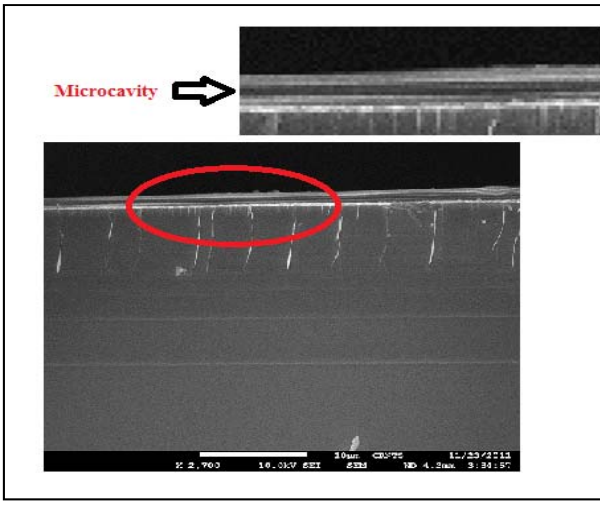

Fig. 5 (b): SEM Cross-sectional view of PSMC Structure

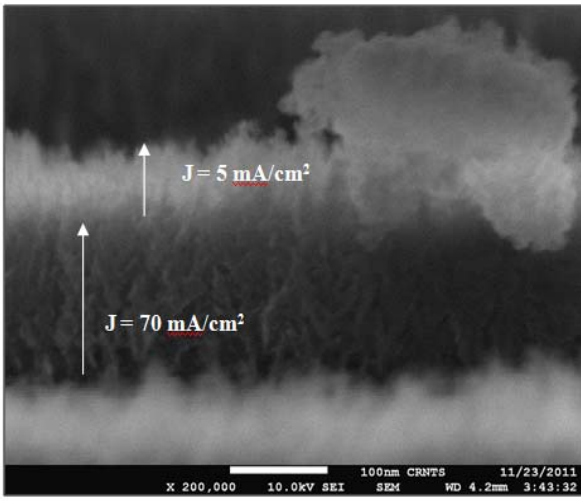

Fig. 5 (c) Low and High Porosity layers of PSMC

In Fig. 5 (c), the light grey stripes are corresponds to low porosity layers (J=5 mA/cm^2, high refractive index) and the dark gray stripes are corresponds to the high porosity layers (J= 70 mA/cm^2, low refractive index). Further, the branched cylindrical structure possessed by the pores, is also clearly visible in Fig. 5 (c); which shows that the pore growth is occurred in the depth (perpendicular to the surface) of the structure.

Optical characterization of the prepared sensor device structure was done using optical spectrometer. Reflectance measurements were done in the air and the polished silicon wafer was used as a reference. A reflectance spectrum of the 1D-PSMC structure is shown in Fig. 6.

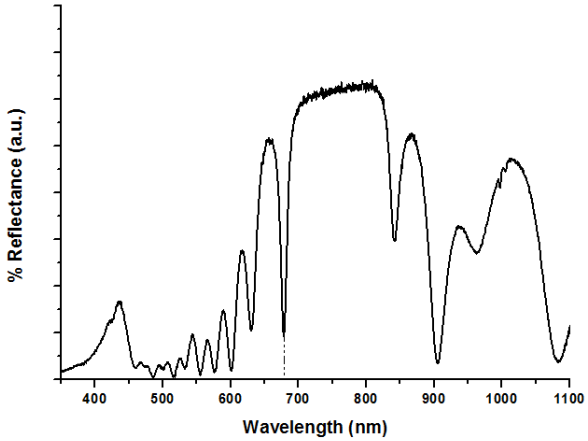

Fig. 6: Reflectance Spectra of PSMC Sensor Device Structures

As shown in Fig. 6, the photonic resonance dip centered at 679 nm is observed in the reflectance spectrum of microcavity structure. The presence of small peaks between 400 to 500 nm was observed in the reflectance spectra of Fig. 6, due to the refractive index dispersion of PS at those high energies [22].

C. Glucose Detection

After fabrication and characterization of 1D-PSMC sensor device, their performance as the optical biosensor device was tested by analysing the wavelength shift in the reflectance spectra during their exposure to different concentrations (2%, 4%, 6%, 8% and 10%) of glucose. Variations in the photonic resonance dip in the reflectance spectra of the sensing device during exposure to different concentrations of glucose are shown in the Fig. 7. During the adsorption,

wavelength in the reflectance spectra promptly shifted toward the higher wavelength (low energy) regions. This phenomenon can be attributed to the capillary adsorption of the glucose molecules within the pores of the porous structure. The wavelength shift measured from the reflectance spectra of 1D-PSMC structures for the different concentrations is listed in Table 1.

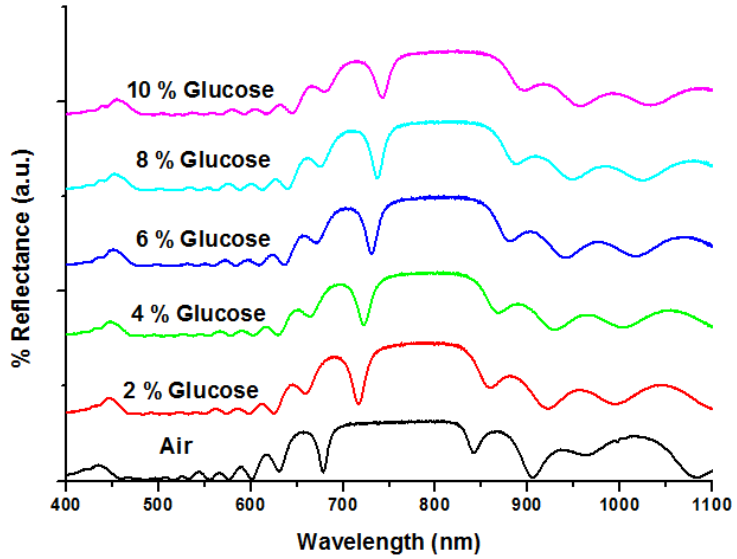

Fig. 7: Wavelength Shift in the Reflectance Spectra of sensor device before and after glucose Adsorption.

Table 1. Wavelength Shift in Reflectance Spectra of 1D-PSMC Structures after Organic Solvents Adsorption

Glucose Concentration (%)	Wavelength Shift (nm)
2	39.52
4	44.83
6	53.22
8	59.40
10	64.69

It is clearly observed from Fig. 7 and Table 1, that the wavelength in the reflectance spectra of the 1D-PSMC sensor device were shifted to higher wavelength, because the pores were filled with glucose molecules ($n > 1.0$). The filled pores with glucose molecules increase the overall effective refractive index and consequently optical thickness of the porous structure. This effect promotes the wavelength shift in the reflectance spectrum. The strength of the wavelength shift depends on the glucose concentrations. Higher the concentrations of glucose, higher the refractive index of the solution and hence, higher the wavelength shift.

The relationship between concentrations of glucose and the wavelength shift is plotted in Fig. 8 from the results of Table 1. Fig. 8 shows the good linear fitting for the graph of the glucose concentrations *vs.* wavelength shift. As shown in the Fig. 8, when the sensor device was exposed to glucose solution of high concentrations, large variations in the reflectance spectra were observed; correspondingly, when the sensor device was exposed to low concentrations solutions, small variations in the reflectance spectra were observed. This is due to the variations in the effective refractive index of the 1D-PSMC layers according to the different concentrations of glucose solution adsorbed in pores. In the Fig. 8, it is observed that all the experimental points are on the linear fitting.

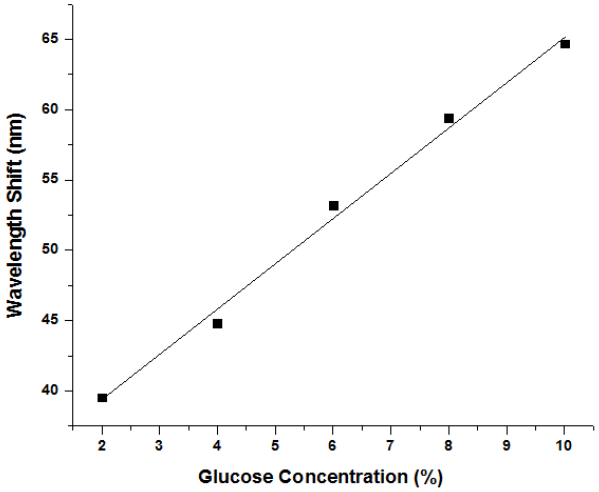

Fig. 8: Refractive Index vs. Wavelength Shift

Sensitivity is one of the most important issues to evaluate the performance of the sensors. In this case, the response of the sensor structure was evaluated throughout the change of the wavelength shift ($\Delta\lambda$) in the reflectance spectrum for different concentrations of glucose solutions. This parameter showed to be a good indicator for sensing measurement in the 1D-PSMC sensing devices. In this sensor device, the measured sensitivity is 3.146 nm/Concentration (%).

Also, our experiment showed that the 1D-PSMC sensor device can also be used as reversible sensor device applications. After each experiment, the glucose molecules inside the porous structure were removed by rinsing the sensor device three times in the ethanol solution. After the rinsing the photonic resonance dip of the sensor device comes to its original position. This feature is very much useful for the development of effective reversible 1D-PSMC glucose biosensor device.

4. Conclusions

To conclude, porous silicon based photonic bandgap microcavity optical sensor device structures were fabricated by electrochemical anodization and proposed as the glucose biosensor devices. Porous structure is confirmed in the plan view of SEM characterization. Large number of pores uniformly distributed on overall surface and multilayered structure with periodic variation of the refractive indices is observed in the SEM characterizations. Optical characterization showed sharp photonic resonance dip, which is important for the accurate measurement of the wavelength shift. Optical sensing of glucose level (2%-10%) is demonstrated using the sensor device. The effective optical thickness and the refractive index of the structure changes due to capillary adsorption of the glucose molecules in the porous structures which results in the wavelength shift in the reflectance spectra. Good linear fitting for the different glucose concentration is obtained. Experiments showed that, after complete removal of the glucose molecules from the porous structure reflectance spectra of the structures promptly returns to their original waveform position. This is a very good quality of these structures, as it is helpful in the development of reversible sensing devices.

Acknowledgments

This work was supported by the grant from Defence Research and Development Organization (DRDO), Govt. of India. Authors are also thankful to CRNTS, SAIF, IIT Bombay for the structural characterization of the samples.

References

[1] G.A. Melikjanyan, Kh.S. Martirosyan, Armenian Journal of Physics **4,** 4 (2011).
[2] G. Piechotta, J. Albers, R. Hintsche, Biosensors and Bioelectronics, **21** (2005).
[3] Kevin J. Cash, and Heather A. Clark, Trends Mol. Med., **632** (2010).
[4] Weiwei Chen, Hui Yao, Chi Hung Tzang, Junjie Zhu, Mengsu Yang, and Shuit-Tong Lee, Appl. Phys. Lett. **88,** 213104 (2006).
[5] Giancarlo C. Righini, Antonella Tajani and Antonello Cutolo (eds.), "An Introduction to Optoelectronic Sensors", World Scientific Publishing Co. Pvt. Ltd., (2009).
[6] A. G. Cullis, L. T. Canham and P. D. J. Calcott, J. Appl. Physics, **82,** 3 (1997).
[7] W. TheiB, Surf. Sci. Rep. **29** (1997).
[8] N. Koshida (ed.), "Device Applications of Silicon Nanocrystals and Nanostructures", Springer Science, 1st Ed., (2009).
[9] P. N. Patel, V. Mishra, A. K. Panchal, Journal of Optoelectronics and Biomedical Materials **4,** 1 (2012).
[10] R. S. Dubey, D. K. Gautam, Chalcogenide Letters **6**, 10 (2009).
[11] M. A. Mahdi, Asmiet Ramizy, Z. Hassan, S. S. Ng, J. J. Hassan, S. J. Kasim, Chalcogenide Letters **9**, 1 (2012).
[12] R. S. Dubey, D. K. Gautam, Journal of Optoelectronic and Biomedical Materials **1**, 1 (2009).
[13] A. Mortezaali, S. Ramezani Sani, F. Javani Jooni, Journal of Non-Oxide Glasses **1**, 3 (2009).
[14] A. Ioanid, M. Dieaconu, S. Antohe, Digest Journal of Nanomaterials and Biostructures **5**, 4 (2010).
[15] E. Tommasi, Luca De Stefano, Ilaria Rea, Valentina Di Sarno, Lucia Rotiroti, Paolo Arcari, Annalisa Lamberti, Carmen Sanges and Ivo Rendina, Sensors, **8**, (2008).
[16] H. Saha, International Journal On Smart Sensing And Intelligent Systems, **1**, 1 (2008).
[17] Luca De Stefano, Ivo Rendina, Luigi Moretti, Stefania Tundo, and Andrea Mario Rossi, Applied Optics, **43**, 1 (2004).
[18] A. K. Panchal, P.G. Kale and C. S. Solanki, ICAER, **797**, (2007).
[19] Huimin Ouyang and Philippe M. Fauchet, SPIE Optics East, **6005**, 600508 (2005).
[20] Han-Jung Kim, Young-You Kim, Ki-Won Lee, Horchhong Cheng and Dong Han Ha, Physica B, **406**, 1536 (2011).
[21] R. Dubey and D. K. Gautam, Opt. Quant. Electron, **41**, 189 (2009).
[22] A. Bardaoui, R. Bchir, H. Hamzaoui and R. Chtourou, Eur. Phys. J. Appl. Phys. **51**, 30701(2010).